Journal of Environmental Chemical Engineering 11 (2023) 109638

Contents lists available at ScienceDirect

Journal of Environmental Chemical Engineering

journal homepage: www.elsevier.com/locate/jece

Dacryodes edulis leaf derived biochar for methylene blue biosorption

Nnaemeka J.N. Nnaji [a,*], Christopher U. Sonde [a], Obianuju L. Nwanji [a], Godwin C. Ezeh [b], Abraham U. Onuigbo [c], Adamma M. Ojukwu [c], Precious C. Mbah [d], Abosede Omowumi Adewumi [e], Edith C. Unoka [f], Jude O. Otedo [f], Thereasa U. Onuegbu [c]

[a] Department of Chemistry, Alex Ekwueme Federal University Ndufu Alike, Ikwo, Ebonyi State, Nigeria
[b] Centre for Energy Research and Development, Obafemi Awolowo University, Ile-Ife, Osun State, Nigeria
[c] Department of Pure and Industrial Chemistry, Nnamdi Azikiwe University, Awka, Anambra State, Nigeria
[d] Department of Biochemistry, Alex Ekwueme Federal University Ndufu Alike, Ikwo, Ebonyi State, Nigeria
[e] Department of Chemical Sciences, Lagos State University of Education, Ijanikin Campus, Lagos State, Nigeria
[f] Department of Industrial Chemistry, Dennis Osadebe University, Asaba, Delta State, Nigeria

ARTICLE INFO

Editor: Stefanos Giannakis

Keywords:
Biochar
Biosorption
Dacryodes edulis
Methylene blue
Regeneration

ABSTRACT

Carbonized *Dacryodes edulis* leaf (CDEL) which was obtained at 250 °C, was used for the biosorption of methylene blue (MB) dye from aqueous solutions. The biosorbent was characterised using Boehm titration, pH of zero point charge (pH_{zpc}), FTIR, SEM, XRD and ED-XRF. Mineral compositions of CDEL revealed good amounts of Fe, Ca and K which are of nutritional importance. The pH at zero point of charge (pH_{zpc}) and specific surface area (SSA) of CDEL were found to be 7.5 and 0.983 m^2/g respectively. Freundlich isotherm gave good fit to equilibrium biosorption data. Elovich kinetic model gave the best fit to kinetic data which is consistent with chemisorption. Scanning electron microscopy (SEM) and infrared spectroscopy (FTIR) revealed effective biosorption processes. Calculated thermodynamic parameters revealed spontaneous and exothermic biosorption of MB onto CDEL. Highest amount of MB was removed at pH 4 and the percentage removal was about 93%; hence, CDEL is a good biosorbent for MB from aqueous solutions. Generally, CDEL exhibited > 70% MB removal after three adsorption-desorption cycles, showing that it is re-usable and a promising biosorbent for the treatment of MB dye contaminated water.

1. Introduction

Clothing is a necessity for the survival of man on earth. In this modern era, textile industries produce many kinds of clothing materials which require dyeing, this is a vital industrial activity. Consequently, industrial effluents from textile industries are usually discharged into nearby streams, rivers and land. Discharge of untreated industrial effluents into the environment is known to be detrimental to fauna, flora and human as well [1]. In like manner, leather and pharmaceutical industries produce dye-polluted wastewaters, making the use of dyes a very important research interest [2]. Textile, leather and pharmaceutical industrial effluents are known to contain methylene blue, a vital dye pollutant which raises environmental concern when not removed before discharge of effluents into nearby environments [2,3]. Consequently, these may affect bacterial growths and photosynthesis of aquatic plants [4]. Literature works [5–9] have reported that methylene blue can cause some harmful effects in humans, such as: increase in heartbeat, vomiting, low oxygen level resulting in cyanosis, jaundice and quadriplegia, and tissue necrosis. Adegoke and Bello [10] in their work opined that the presence of dyes in water bodies cause micro-toxicity in fishes because they can sequester metal ions.

Polluted industrial effluents in a developing country such as Nigeria, have greater chances of being disposed into nearby environments with little or no treatments because regulatory agencies do little or nothing in this regard [3]. Poverty is another important factor that cause the inability of industries in developing nations to put in place facilities for effluent purification. Technologies abound for the treatment of dye-contaminated industrial efflents [11–13], but biosorption seems the commonest method of treating aqueous effluents because of low biosorbent regeneration cost and equipment for biosorption processes are easily availabile [14]. It is of uttermost importance to use low cost, easily available and environmental friendly materials as biosorbents for

* Corresponding author.
E-mail address: joemeks4u@yahoo.com (N.J.N. Nnaji).

https://doi.org/10.1016/j.jece.2023.109638
Received 17 December 2022; Received in revised form 15 February 2023; Accepted 3 March 2023
Available online 7 March 2023

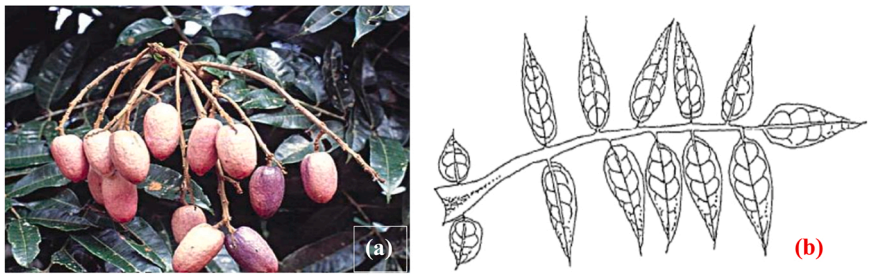

Fig. 1. Fruits of *D. edulis* (a) and leaf of *D. edulis* [35].

removal of dye colour from effluents; agricultural waste materials are known to fulfil these conditions. The use of agricultural waste materials has presently attracted wide application/attention for treatment of industrial wastewaters [15]. This is because as biosorbents, their application is less sophisticated, effective, efficient, easily available and economical [13,14]. The potentials of agricultural waste materials have been assessed for the removal of methylene blue dye. Examples include: the evaluation of *Carica papaya* and defatted *Carica papaya* seeds as novel non-conventionl lowcost biosorbents for the removal of methylene blue [16,17]. Other biosorbents used in the removal of methylene blue are modified cashewnut testa tannins [3], *Paspalum notatum* [18], guava leaf powder, gulmohar plant leaf powder, palm kernel fibre, dehydrated peanut hull, hazelnut shells, yellow passion fruit waste and wheat shells [19–24]. Removal of methylene blue from aqueous solution by biosorption has been reported by Shakoor and Nasar [25] using corn cobs, garlic peel, hazelnut shell, jack fruit peel, longan shell, pineapple stem and spent tea leaves. Banana fibre, coconut fibre and sawdust were reported earlier for methylene blue removal from water by Karthik and co−workers [26]. Agricultural waste can be converted to materials whose surface areas and adsorption capacities are expected to be improved; such materials include: biochar, hydrochar, activated charcoal, nano particles and nano composites. The investigated single and binary systems for the removal of amoxicillin (AMX) and tetracycline (TCN) using activated carbon derived from durian shell has appeared in literature [27]. Thue and co−workers [28] reported the use of activated carbon derived from sapelli wood sawdust for o-cresol adsorption. Motivation for this work is principally derived from these earlier works.

Nigeria produces huge amounts of agricultural wastes due to availability of large vegetation lands; regrettably, little use of these agricultural waste materials are made [3].

Review works [29,30] highlighted the importance of biochars, particularly as applied to wastewater treatments by biosorption. This has necessitated the use of CDEL for the removal of methylene blue from aqueous solutions. *Dacryodes edulis* is a tree which originated from Central Africa and Gulf of Guinea area, areas of equatorial and humid tropic climates [31]. Parts of the tree, fruits and leaf, are presented in Fig. 1. An earlier work reported the phytochemical constituents of D. edulis leaf as saponins, alkaloids, tannins, flavonoids and phenolic compounds [32]. The only work on the use of biosorbent derived from *Dacryodes edulis* leaf (CDEL) was reported on the removal of crude oil from water [33]. This study therefore presents the application of an agricultural waste material, *Dacryodes edulis* leaf from which biochar was derived for the removal of MB from aqueous solutions. This work suggests the usefulness of this agricultural waste as biosorbent with the aim to solve waste problems in Nigeria, elaborate its use as lowcost biosorbent for wealth creation and meet regulatory standards for treatment of industrial wastewaters.

The use of CDEL for the removal of methylene blue from aqueous solutions has not been reported before in literature; this work therefore, seeks to fill this vital gap. Agricultural byproducts abound in Nigeria, much of which are regarded as wastes and usually underutilised as very few are used in domestic activities such as cooking fuels. DEL, an agricultural byproduct, has found little or no useful application in Nigeria. This study therefore presents the characterisation and application of its carbonized form as a viable biosorbent for the treatment of wastewaters containing organic contaminants such as dyes. Our choice of studying the methylene blue biosorption properties of CDEL was because of enhanced surface area and porosity properties of biochar compared to the biomass [34].

2. Materials and methods

2.1. Biosorbent preparation

Dacryodes edulis leaf (DEL) samples were used as starting materials for the purification of laboratory simulated textile industrial waste water. DEL was collected under trees in Nsukka and identified by the curator of the herbarium at Department of Plant Science and Biotechnology, University of Nigeria Nsukka. Collected samples were washed in distilled water and air dried (during harmattan) for three weeks. The dried biomass was ground with a food processor (Moulinex, France). This was placed in a crucible rack covered with lids and transferred gently to a muffle furnace at a temperature of 250 °C for three hours. Similar biochar preparation conditions, temperature and time, have been reported earlier [36–38] and the purpose of choosing 250 °C was to reduce ash content and to increase MB biosorption [39]. The crucible containing the carbonized sample was removed from the crucible rack and then kept in the desiccator at room temperature of 27 °C. At the end of the process, Carbonized *Dacryodes edulis* leaf (CDEL) was ground to powder using a laboratory mortar and pestle, sieved through a 150 μm mesh size and stored in air-tight container.

2.2. Biosorbent characterisation

Surface chemistry of CDEL biosorbent was characterized by adopting Boehm titration and pH drift (or pHzpc—pH at zero point of charge). Boehm titration method is described as follows: 0.5 g of ground CDEL were dispersed in 50 mL each of 0.05 M solutions of $NaHCO_3$, Na_2CO_3, NaOH and HCl contained in 250 mL glass bottles. The bottles were shaken using a mechanical shaker (180 rpm) for 24 h. After 24 h, the samples were filtered using whatman No.1 filter paper and titrated with 0.05 M NaOH or 0.05 M HCl depending on the starting solution used. The amount of acidic groups on the surface of the CDEL were approximately calculated as follows: $NaHCO_3$ (carboxylic group), Na_2CO_3 (carboxylic and lactonic groups) and NaOH (carboxylic, lactonic and phenolic groups). The number of surface basic sites was calculated from the amount of HCl that reacted with the filtrate.

The method used for determination of pH at zero point of charge (pHzpc) of CDEL adsorbent is described as follows: 50 mL of 0.01 M KCl were prepared and added into a series of glass bottles with corks. Their pH values were adjusted in range between 2 and 10 at interval of 0.5 using either 0.1 M HCl or 0.1 M NaOH. The pH of initial solutions were measured with a pH meter and noted as $pH_{initial}$. Afterwards, 0.15 g of the ground CDEL sample was added to each bottle and corked. This set up was shaken for 48 h after which the second pH values of the extracts noted as pH_{final} were measured with a pH meter. A plot of the difference

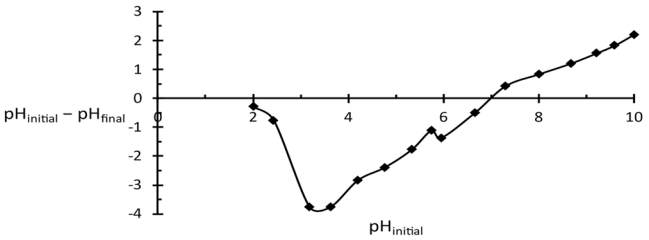

Fig. 2. pH_{zpc} of CDEL.

between $pH_{initial}$ and pH_{final} on the *y*-axis versus the $pH_{initial}$ on the *x*-axis was made as shown in Fig. 2. The zero−point charge pH was the point where the curve cuts the *x*-axis.

The specific surface area (SSA) of CDEL adsorbent was calculated from the following equation [40]:

$$SSA = \frac{[MB]_{absorb} \times 6.02 \times 10^{23} \times 130\left(\frac{0}{A}\right)^2}{319.98 \times M_s} \quad (1)$$

where SSA is the specific surface area (m^2g^{-1}), $[MB]_{absorb}$ is the concentration of absorbed MB (g/L), M_s is mass of CDEL (g), $\left(\frac{0}{A}\right)^2$ is Armstrong unit (x 10^{-10} m).

FTIR spectra of native CDEL and MB absorbed CDEL were recorded, by KBr method, using SHIMADZU FTIR-8400S in the vibrational absorption range of 4000–500 cm^{-1}.

Energy dispersive X-ray fluorescence (ED−XRF) technique was used to determine the mineral content of CDEL [41] using portable AMPTEK (R).

The surfaces of native CDEL and MB absorbed CDEL were captured by scanning electron microscopy, a Phenom World model.

2.3. Biosorption experiments

MB was used as model textile dye. A stock solution (1000 mg/L) of MB was prepared by dissolving an appropriate amount of dye in distilled water. Other concentrations were freshly prepared by diluting this stock dye solution.

The effect of experimental parameters such as initial dye concentration (2, 4, 6, 8, 10, 20, 40, 60, 80 and 100 mg/L), biosorbent dose (1, 2, 4, 6, 8 and 10 g), pH (2, 4, 6, 8 and 10), temperature (30, 40, 50, 60 and 70 °C) and contact time (5, 10, 20, 30, 60 and 120 min) were studied for the sorption of MB onto CDEL. Other parameters such as pressure, stirring speed and volume were constant for all batches. For adjusting the pH, 0.1 M solutions of NaOH and HCl were used. For biosorption process, 100 mL of solutions were put in conical flasks and placed on a magnetic stirrer. Afterwards, the flasks were removed and the solutions filtered through Whatman No. 1 filter paper and subsequently, the dye concentrations were determined using a UV/visible spectrophotometer (UNICO). The concentrations of dye solutions unadsorbed were obtained using a calibration curve.

The biosorption capacity at different time intervals were calculated from the following relationship [3]:

$$q_t = \frac{V(C_0 - C_t)}{m} \quad (2)$$

where C_0 and C_t are the initial methylene blue concentration and the methylene blue concentration after different time intervals (mg/L)

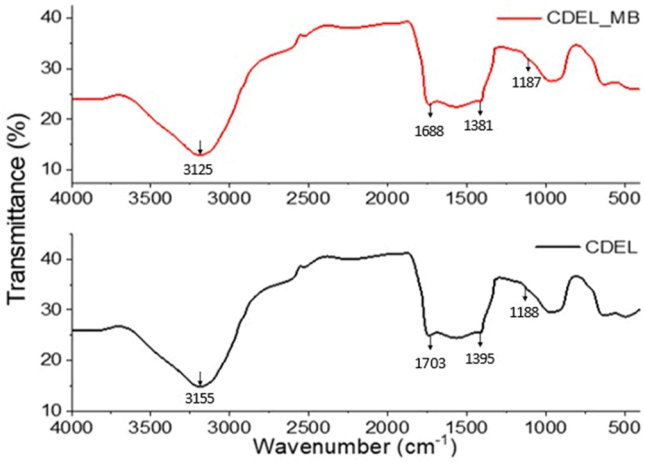

Fig. 3. FTIR spectra of: a) CDEL native and b) MB biosorbed CDEL.

respectively, V is the volume of dye solution used (L) and m is the mass of the biosorbent (g).

The equilibrium biosorption capacity was calculated from the following relationship [3]:

$$q_e = \frac{V(C_0 - C_e)}{m} \quad (3)$$

where C_e is the equilibrium dye concentration (mg/L).

Concentrations of the MB dye, in the range 0–200 mg/L, were prepared from stock solution and read on a UV/visible spectrophotometer. A calibration curve of absorbance against MB dye concentrations was obtained from standard MB dye solutions of known concentrations. As such, obtained calibration curve fitted a straight line with a high correlation coefficient ($r^2 = 0.9931$) and suggests that the molar absorptivity is constant over the concentration range investigated. This implies that the MB dye concentration will be determined with good precision [17].

2.4. Desorption experiments

MB desorption was studied in 100 mL solutions of distilled water and ethanol solutions were used to desorb MB biosorbed biochar samples, according to the isothermal biosorption experiments above. The solutions were stirred for 24 h. Also, the recyclability of CDEL was evaluated three times. These desorption experiments were conducted so as to show reduced cost of biosorption process using CDEL.

3. Results and discussion

3.1. Biosorbent characterisation

The surface of CDEL contains phytochemicals in the form of hydrogen, oxygen and nitrogen. Phytochemicals are known to affect the surface chemistry of materials [17]. Surface chemistry basically involves the probing of the acidity and basicity of CDEL. Functional groups such as −COOH, lactonic and phenolic groups which make-up the surface material acidity, and the surface material basicity includes oxygen-containing groups and lattice oxygens characterized as Lewis basic sites [17]. Surface chemistry analyses of CDEL biosorbent is

Table 1
Surface Chemistry values.

Sample	Carboxylic	Lactonic	Phenolic	Acidic value	Basic value	pH	pH_{zpc}	SSA
mequiv.g^{-1} of CDEL biosorbent								
CDEL	0.162	0.538	0.950	1.650	1.700	7.6	7.5	0.983 m^2/g

Table 2
Mineral content characterization of CDEL by X − ray fluorescence analysis.

Elements	Conc Value	Conc Error	Unit
K	5976	±106	Ppm
Ca	1.7506	±0.0182	wt%
Ti	175	±18	Ppm
Cr	174	±18	Ppm
Mn	613	±34	Ppm
Fe	1.3532	±0.0100	wt%
Ni	1058	±45	Ppm
Cu	1614	±55	Ppm
Zn	1338	±50	Ppm
Rb	287	±23	Ppm
V	42	±9	Ppm
Se	320	±25	Ppm
Co	506	±31	Ppm
Mo	158	±17	Ppm

Table 3
Elemental composition results from EDX.

Native_CDEL		
Element Symbol	Element Name	Concentration (%)
C	Carbon	22.5 ± 0.6
N	Nitrogen	53.1 ± 1.0
Rb	Rubidium	14.8 ± 1.6
O	Oxygen	9.6 ± 3.6
MB_CDEL		
Element Symbol	**Element Name**	**Concentration**
C	Carbon	21.5 ± 0.7
N	Nitrogen	50.2 ± 1.3
Rb	Rubidium	7.6 ± 3.6
O	Oxygen	12.2 ± 2.5
Am	Americium	8.5 ± 2.3

presented in Table 1, showing the amount of acidic and basic functional groups.

The pH_{zpc}, otherwise known as pH at zero point of charge was also determined and presented in Fig. 2. The pH_{zpc} of 7.5 shown by the CDEL biosorbent is consistent with the Boehm titration result that presented dominance of basic group of the CDEL surface.

Fig. 3 presents the FTIR spectra of native and MB biosorbed CDEL in the range of 500–4000 cm^{-1}. Signals around 3155 cm^{-1} (native) which shifted to 3125 cm^{-1} (MB biosorbed) indicates -OH and -NH functional groups. Presence of C═O of lignin (in CDEL) can be attributed to the following observed signals: 1703 cm^{-1} (native CDEL) changed to 1688 cm^{-1} (MB biosorbed CDEL). The signals of C-H vibrations of cellulose was observed to change from 1395 to 1381 cm^{-1} for native CDEL and MB biosorbed CDEL respectively. There are signals at 1188 cm^{-1} for both native and MB biosorbed CDEL which can be attributed to C-O and C-O-C vibrations. The observations are consistent with reports found elsewhere [42].

The mineral compositions of CDEL are presented in Table 2 and reveal the presence Fe, Ca, K, and the likes. This suggests that CDEL is a vital source of iron, calcium and potassium which are of nutritional importance [43]. EDX results are presented in Table 3 and Fig. 4, these show that CDEL contains Rb which also appears in XRF result of Table 2. Rubidium is a vital microelement which can kill and inhibit bacteria. Gels containing Rb–Ca are used in/for diabetic wound dressings [44]. Considering that CDEL contains high quantity of calcium (Table 2) and low quantity of rubidium (Table 3), the use of CDEL as biosorbent would very likely be environmentally friendly.

SEM images of native CDEL and MB loaded CDEL are presented in Fig. 5. In Fig. 5a, CDEL surface shows irregular and rough layered pores. But Fig. 5b presents a changed surface for MB biosorbed CDEL revealing most rough layered pores to be covered. When compared to native CDEL, the rough but smoother surface structure of MB loaded CDEL indicats surface coverage with molecular cloud of dye.

The pore size distribution of CDEL is presented in Fig. 6 and is consistent majorly with macroporous material characteristics (> 50 nm) [45].

TGA curve of CDEL is presented in Fig. 7. The temperature range of 50–100 °C shows initial weight loss which is due to water content evaporation. About 42% weight loss can be seen within 100 − 300 °C temperature range. This region shows marked decomposition/degradation of CDEL components, cellulose and lignin (as infrared spectroscopic analyses suggests). This temperature decomposition profile is similar to an earlier reported cellulosic material [46,47].

Fig. 8 presents diffractogram peaks of CDEL. Amorphous nature of native and MB biosorbed CDEL can be seen at 32 ° (2θ) which can be ascribed to cellulose [46] and in perfect agreement with infrared vibrations observed in earlier section. Diffractogram peaks at 44 and 53 ° (2θ) have earlier been reported for magnetite (Fe_3O_4) and maghemite ($\gamma - Fe_2O_3$) [48]. This is excellently corroborated by the high iron content of CDEL from XRF measurement (Table 2). A new difractogram peak appears around 74° (2θ) and suggest very good methylene blue biosorption.

3.2. *Effect of initial concentration and equilibrium studies*

Effect of initial concentration for MB biosorption onto CDEL is presented in Fig. 9. The amount of MB removed increased with increase in initial concentration. Similar result has been reported for MB biosorption onto defatted *Carica papaya* seeds [17]. It has been suggested that this trend is due to the increase in the driving force of the concentration gradient [49].

Graphical plot, Fig. 9, depicting the experimental data was used to determine equilibrium sorption isotherms represented by equations below. Herein, three isotherm equations are presented as follows [4–6, 10,11,49,50]:

Langmuir

$$\frac{C_e}{q_e} = \frac{1}{q_0(b)} + \frac{C_e}{q_0} \tag{4}$$

Freundlich

$$\ln q_e = \ln K_F + \frac{1}{n} \ln C_e \tag{5}$$

Temkin

$$q_e = B \ln A + B \ln C_e \tag{6}$$

where q_e (mg/g) and C_e (mg/L) are the dye amount adsorbed per unit biosorbent weight and concentration of unadsorbed dye in solution at equilibrium, respectively. K_L is the Langmuir constant, q_0 is Langmuir (theoretical) saturation capacity, K_F is the Freundlich constant, "n" is the Freundlich constant which explains the heterogeneity of the biosorbent, and Temkin constants are represented by A and B.

Langmuir isotherm assumes a monolayer sorption on a surface which has binding sites of uniform energy values because they are similar and are non-interacting. Values of Langmuir constant and Langmuir theoretical monolayer saturation capacity obtained are $q_0 = 7.911$ mg/g obtained and $b = 0.334$ L/mg respectively. These are determined respectively from the slope and intercept of the Langmuir isotherm plot, with high coefficient of determination value (0.9517). There is a Langmuir dimensionless constant (R_L), otherwise known as separation factor, which was determined using the following equation [3].

$$R_L = \frac{1}{1 + b(C_0)} \tag{8}$$

where b is a Langmuir monolayer saturation capacity (0.334 L/mg) and Co is initial dye concentration. Plot of Eq. 8 is presented in Fig. S1 (Supplementary information Fig. 1).

Values of calculated R_L are less than unity but more than zero

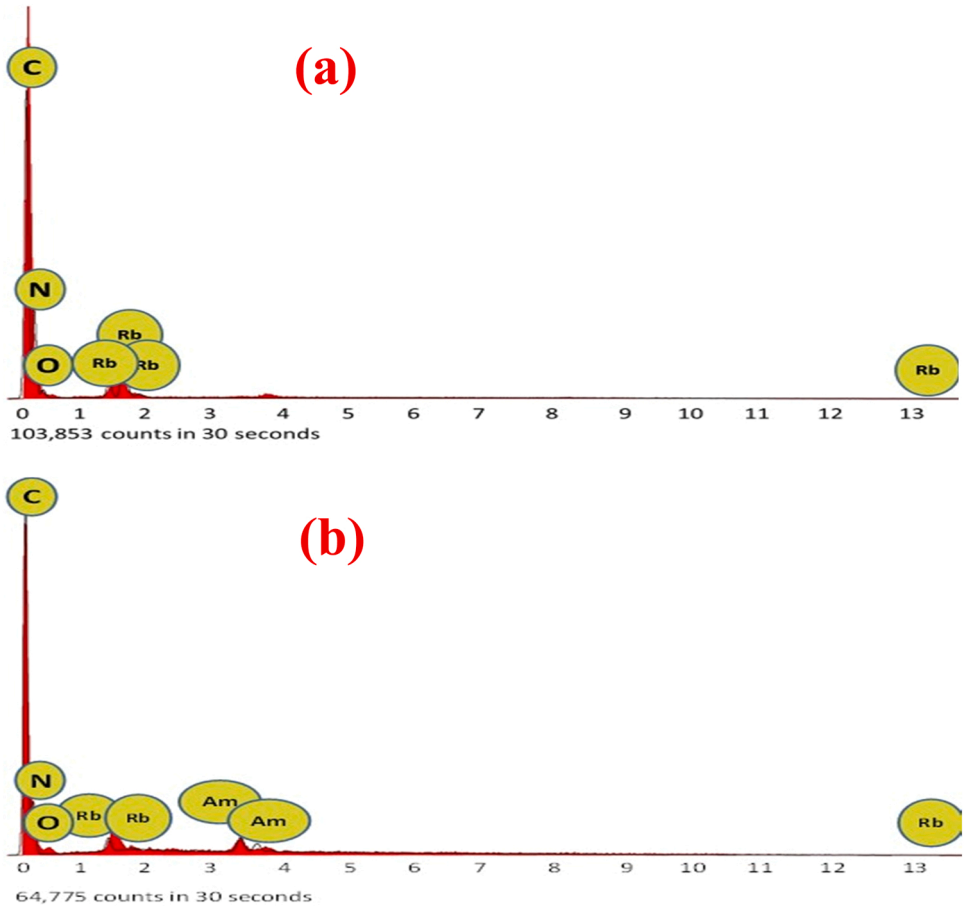

Fig. 4. EDX of: a) native CDEL and b) MB biosorbed CDEL.

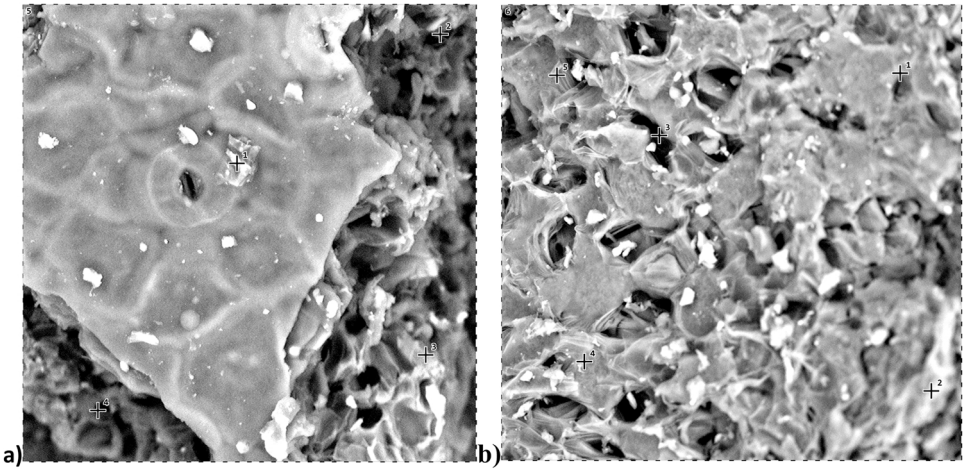

Fig. 5. SEM of: a) native CDEL and b) MB biosorbed CDEL.

suggesting a favourable MB biosorption onto CDEL [50].

Freundlich isotherm assumes a multilayer sorption on a surface with dissimilar binding sites; therefore, it possesses non-uniform energy values. Freundlich plot gave values of Freundlich constants K_F = 1.714 mg/g and n = 2.414 g/L, respectively from intercept and slope, and a high coefficient of determination value (0.972) was obtained.

The Temkin isotherm also assumes a multilayer sorption but differs from the Freundlich mechanism because it assumes that the biosorbent binding sites possess logarithmic energies. Plot of Temkin isotherm gave constants B = 0.785 L/g and A = 45.630 g/L, determined respectively from the slope and intercept with coefficient of determination value (0.7579).

Freundlich isotherm gave the best fit, Fig. S2. This opinion stems from the fact that the least error was calculated for the Freundlich isotherm using the Chi-square statistic (χ^2), Eq. 9 [3].

$$\chi^2 = \sum \left[\frac{\left(q_{e,\exp} - q_{e,cal}\right)^2}{q_{e,cal}} \right] \tag{9}$$

Biosorption influenced by phytochemicals have been reported earlier

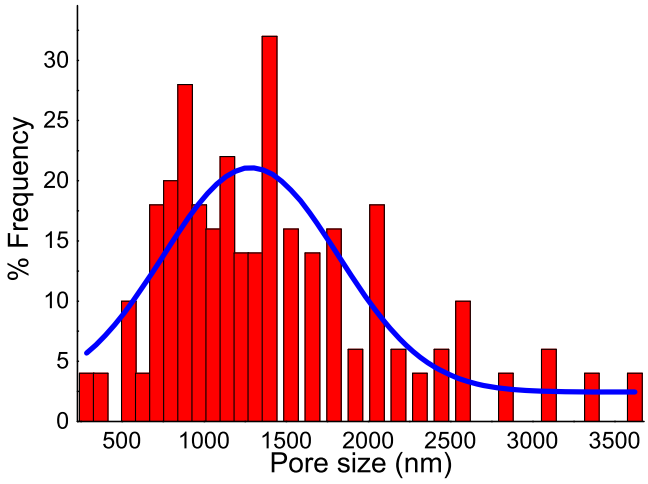

Fig. 6. CDEL pore diameter.

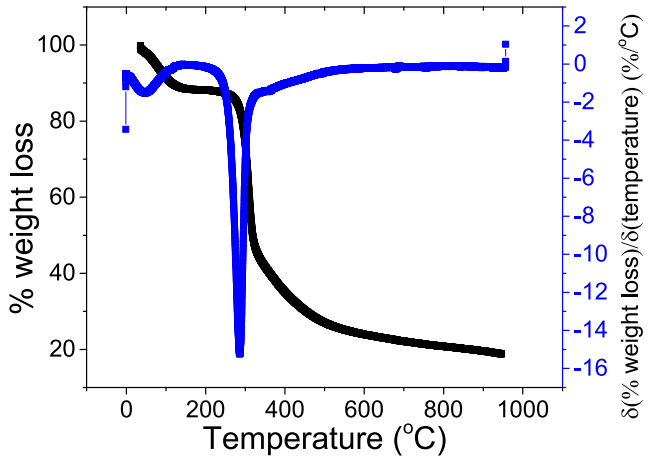

Fig. 7. TGA/DTG curves of CDEL.

to follow Freundlich isotherm [51].

3.3. Effect of biosorbent dosage

The effect of CDEL dosage on the uptake of methylene blue from aqueous solution was monitored by measuring the amount of MB biosorbed from a 100 mg/L solution onto different studied CDEL doses. The sorption curve derived is presented in Fig. 10 and reveals the relationship CDEL dosage has with amount of MB dye biosorbed, which shows that the percentage MB dye biosorbed increased when dosage of CDEL was increased. In contrast, the observed trend for equilibrium adsorption capacity (q_e) shows a decrease when CDEL dosage increase, such that 1–10 g/L dosage increase led to a 6.60–0.773 mg/g decrease of equilibrium adsorption capacity. The observed trend is that increased CDEL dosage caused MB percentage removal to increase due to increased surface area which consequently, increased number of available biosorption sites. The same trend has been observed by Hameed [52]. However, the adsorption capacity was found to decrease, from 6.60 – 0.773 mg/g, most likely because of decrease in liquid–solid ratio.

The equilibrium adsorption capacity (q_e) has a relationship with CDEL dose, Fig. S3, with a coefficient of linear regression ($r^2 = 0.7115$) as represented below [50]:

$$q_e = S(BD_{CDEL}) + Y \quad (10)$$

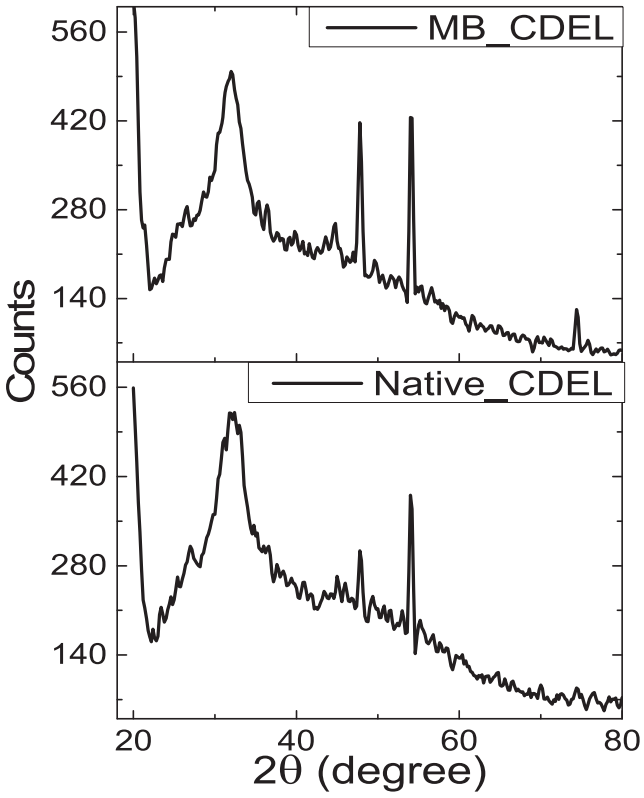

Fig. 8. XRD diffractograms of studied biosorbents.

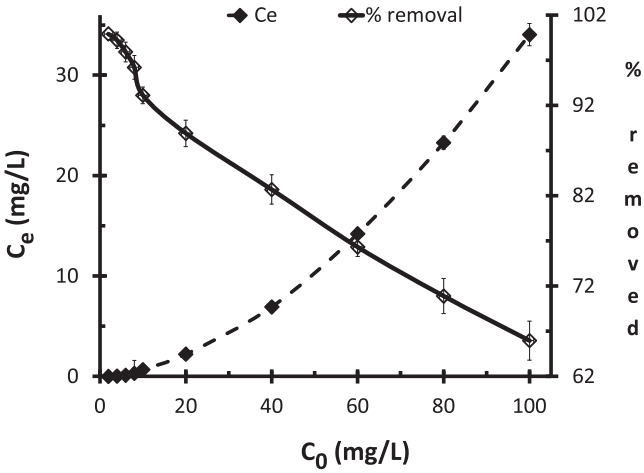

Fig. 9. Effect of concentration on MB biosorption onto CDEL (pH = 4, time = 30 min, dosage = 1 g/100 mL, temperature = 29 °C).

where BD_{CDEL} is the biosorbent dosage, the constant "Y" is the maximum sorption capacity of CDEL, and the slope "S" is related to the adsorption potential of CDEL. The negative value of S stems from the fact that equilibrium adsorption capacity decreased with increase in CDEL dose [50].

3.4. Effect of initial pH

To understand the biosorption mechanism of CDEL, knowledge of the pH_{zpc} is vital. This is because Dawodu and Godfrey [40] opined that at pH values lower than the pH_{zpc}, sorbent surfaces become positively charged favouring biosorption of anionic species. However, at pH values

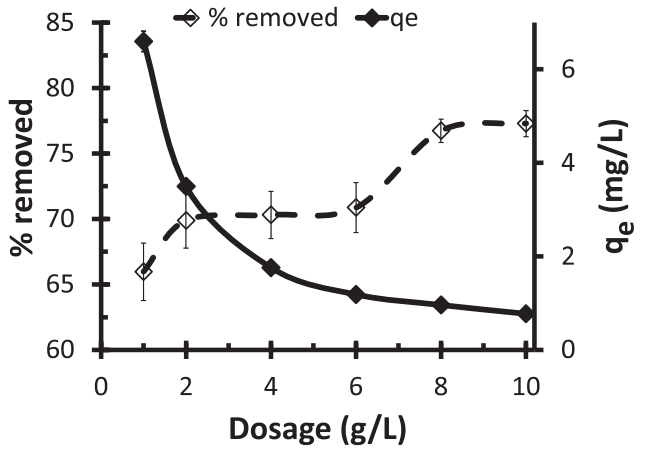

Fig. 10. Effect of CDEL biosorbent on the biosorption of MB dye onto CDEL adsorbent (adsorbent dose: 1–10 g/L, contact time: 60 min, pH: 7.6, Initial MB dye concentration 100 mg/L).

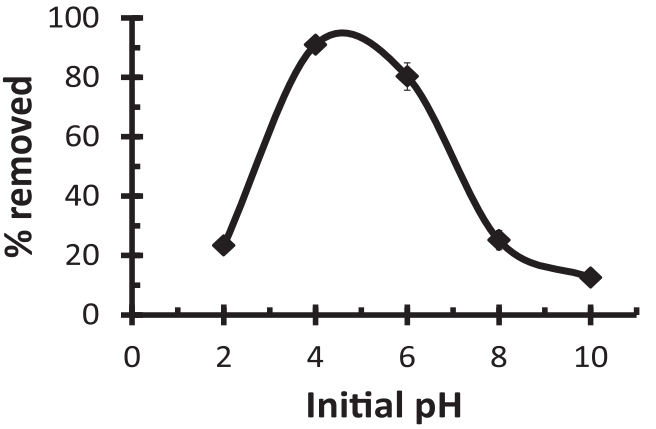

Fig. 11. Effect of initial pH on MB biosorption onto CDEL (Concentration = 100 mg/L, time = 60 min, dosage = 10 g/L, Temperature = 29 °C).

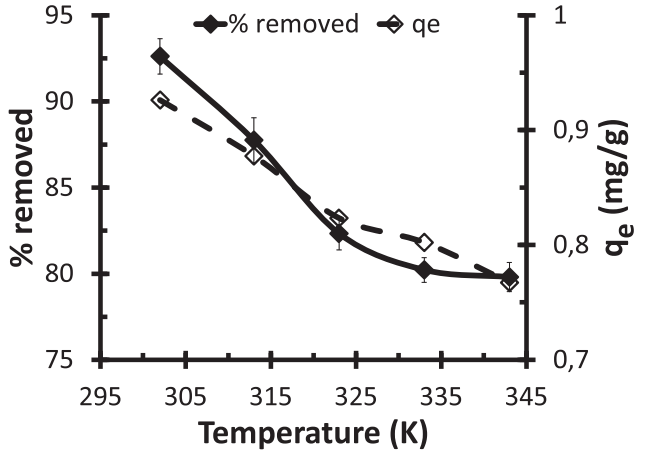

Fig. 12. Effect of temperature on MB biosorption onto CDEL (pH = 4, concentration = 100 mg/L, dosage = 10 g/L and time = 30 min).

higher than the pH_{zpc}, sorbent surfaces become negatively charged favouring biosorption of cations. The pH_{zpc} of CDEL was found to be 7.5 and the slurry pH is 7.6 which is very close to the pH_{zpc}. Therefore, the biosorption of MB onto CDEL is expected not to be favoured in environments at high basic pH because of the structure of MB chloride ions

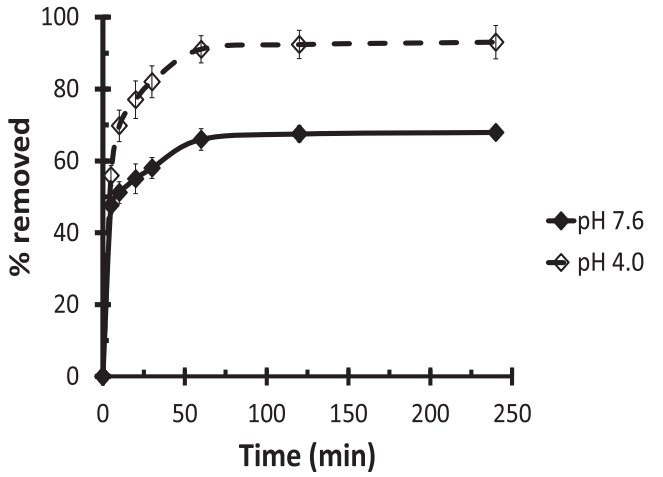

Fig. 13. Effect of time on MB biosorption onto CDEL (concentration = 100 mg/L, temperature = 29 °C, dosage = 10 g/L).

(Cl^-). Fig. 11 presents this trend.

It was observed that highest MB biosorption onto CDEL was obtained at pH value of 4. At pH 4–6 range, MB biosorption onto CDEL gave removal efficiency of about 70% and above. Low biosorption of MB was observed at pH values less than 4 and at pH values more than 6. Consequently, biosorption of MB onto CDEL is pH dependent. Similar results were reported for biosorption of complex dyes onto pine sawdust [42].

3.5. Effect of temperature and thermodynamic considerations

The effect of temperature on CDEL's biosorption of MB from aqueous solutions, containing 100 mg/L dye, was studied and presented in Fig. 12. It was observed that increasing the temperature, decreased the biosorption performance of CDEL, also equilibrium adsorption capacity (q_e) decreased from 0.926 to 0.767 mg/g as temperature increased from 29 °C to 70 °C. The same trend has been observed by Sumanjit et al. [53].

Thermodynamic parameters such as Gibbs free energy (ΔG), the enthalpy change (ΔH), and entropy (ΔS) were calculated using the following equations [11,13]:

$$\ln K_{eq} = \frac{-\Delta H}{RT} + \frac{\Delta S}{R} \tag{11}$$

$$K_{eq} = \frac{q_e}{C_e} \tag{12}$$

and.

$$\Delta G = -\Delta H + T\Delta S \tag{13}$$

where K_{eq} is the distribution coefficient, q_e is the amount of biosorbed dye at equilibrium (mg/g), C_e is the concentration of the dye solution at equilibrium (mg/L), R is the ideal gas constant (8.314 $JK^{-1}mol^{-1}$) and T is the temperature in Kelvin. Plot of Eq. 11 enabled the calculations of change in enthalpy (from slope) and change in entropy (from intercept).

Obtained values of thermodynamic parameters, reveal that MB biosorption onto CDEL gave: negative change in enthalpy value (−27.722 $kJmol^{-1}$), negative change in entropy value (−0.110 $Jmol^{-1}$) and negative Gibb's free energy values at all studied temperatures [− 5.494 $kJmol^{-1}$ (303 K), − 6.703 $kJmol^{-1}$ (313 K), − 7.803 $kJmol^{-1}$ (323 K), − 8.903 $kJmol^{-1}$ (333 K), and − 10.003 $kJmol^{-1}$ (343 K)]. Calculated thermodynamic values suggest that MB biosorption onto CDEL was exothermic, ordered and spontaneous.

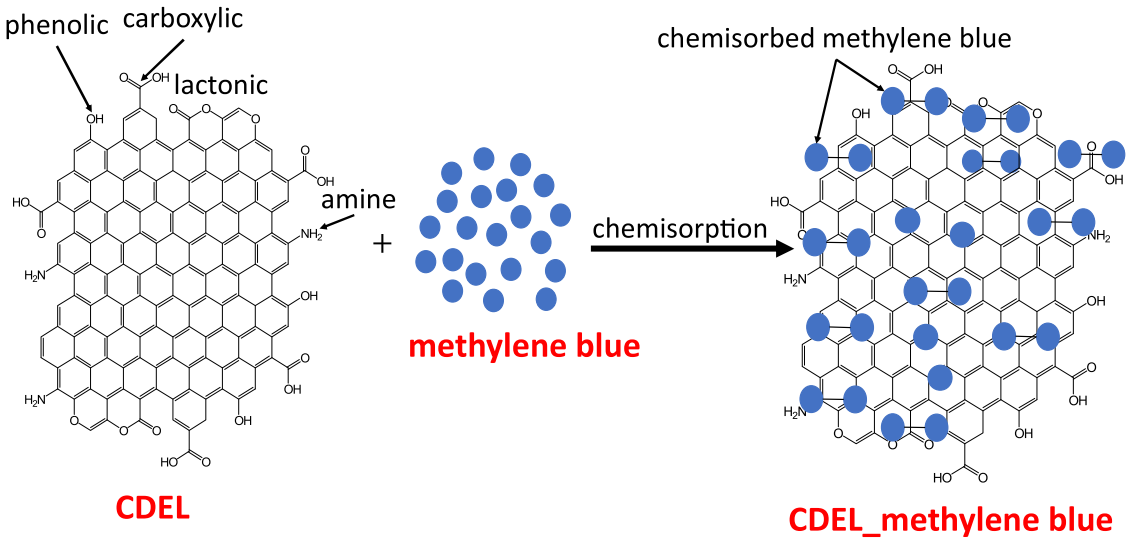

Fig. 14. Proposed biosorption mechanism of CDEL.

3.6. Effect of time and kinetics of MB biosorption

Fig. 13 presents the effect of time for the biosorption of MB onto CDEL, it was found increasing biosorption time increased MB biosorption on CDEL.

The practical importance of understanding the kinetics of MB biosorption onto CDEL cannot be over-estimated, particularly, in process designs and scale-up procedures [2]. Herein, the pseudo-first order, pseudo-second order, intraparticle diffusion and Elovich kinetic models were applied to investigate the biosorption kinetics as shown in Eqs. 14–17 respectively [3]:

$$\ln(q_e - q_t) = \ln q_e - k_1 t \tag{14}$$

$$\frac{t}{q_t} = \frac{1}{k_2 q_e^2} + \frac{t}{q_e} \tag{15}$$

$$q_t = k_i \sqrt{t} + C \tag{16}$$

$$q_t = \frac{1}{\beta} \ln(\alpha\beta) + \frac{1}{\beta} \ln t \tag{17}$$

where k_1, k_2 and k_i respectively are the constants of pseudo-first, pseudo-second order and intraparticle diffusion sorptions. An empirical constant, C, derived from intraparticle diffusion is an integration constant that describes biosorption mechanism. Elovich kinetic model enables the determination of initial adsorption rate constant, α, and another kinetic parameter derived from it, β, which relates to the extent of surface coverage and activation energy for chemisorption. The determined model parameters and constants are given in Table 3.

Plots of Eqs. 14–17 are presented in Fig. S5. Though the kinetic data of MB biosorption on CDEL measured gave highest R^2 values for the pseudo-second order kinetic, it does not reflect the biosorption kinetics at studied pH conditions. As earlier opined by Ani and co−workers [1], using R^2 as predictor of how well a model describes experimental data is misleading. Therefore, the kinetic model which gave the best fit was determined using the χ^2 error statistic, Eq. 9. The values calculated are presented in Table 3 and from the smallest error values calculated, Elovich kinetic model gave good descriptions of the kinetic biosorption at pH 4.0 and 7.6. This suggests that MB biosorption on CDEL followed chemisorption onto CDEL pore surfaces. Similar result was obtained by Fatih [2]. This explains why, MB biosorption onto CDEL is exothermic, result from thermodynamic study result.

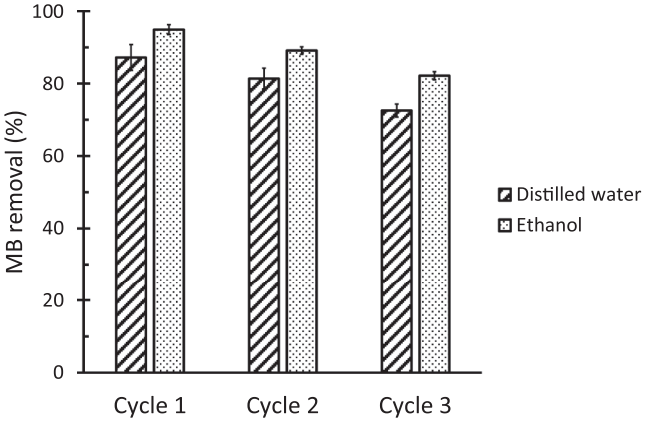

Fig. 15. Desorption results.

3.7. Mechanism of biosorption

Functional groups on CDEL are those determined from Boehm's titration and the results are presented in Table 1. The functional groups presented in Table, from Boehm's titration, are consistent with those of saponins, alkaloids, tannins, flavonoids and phenolic compounds, reported earlier [32]. Seemingly, the chemisorption occurred at the early biosorption stage and supported by Elovich kinetic model, presented in Table 3 by the smallest error obtained from experimental and theoretical kinetic data compared. Apparently, the functional groups possessed by CDEL, Fig. 14, encouraged the chemisorption interaction between electron rich sites of CDEL containing hetero−atoms and the cationic MB molecules. Proposed biosorption mechanism of CDEL is presented in Fig. 14 and involves chemisorption of MB molecules' transfer onto the biosorbent surface, as predicted by the kinetic studies.

3.8. Desorption experiments

Regeneration ability of a biosorbent is vital in considering the cost effectiveness and applicability for usage at industrial scale. Results obtained from CDEL reusability or MB desorption is shown in Fig. 15. It appears that in Fig. 15, ethanol is a better desorbing agent of MB than water. MB removal using distilled water ranged from 87.2 – 72.5% going from cycle 1 to cycle 3, but 94.9 – 82.2% range was obtained when MB was removed from CDEL using ethanol.

Table 4
Kinetic parameters of MB biosorption onto CDEL.

Pseudo-first order					
	k_1	$q_{e,cal}$	$q_{e,exp}$	R^2	χ^2
pH 4.0	0.0270	0.298	0.940	0.9023	23.469
pH 7.6	0.0246	0.214	0.689	0.9443	21.069
Pseudo-second order					
	k_2	$q_{e,cal}$	$q_{e,exp}$	R^2	χ^2
pH 4.0	0.956	0.258	0.940	0.9999	11.211
pH 7.6	0.701	0.333	0.689	0.9998	2.575
Intraparticle diffusion					
	k_i	C		R^2	χ^2
pH 4.0	0.0249	0.627		0.7127	3.013
pH 7.6	0.0163	0.477		0.8343	1.190
Elovich					
	α	B		R^2	χ^2
pH 4.0	10.688	10.235		0.9126	0.012
pH 7.6	32.022	16.556		0.9588	0.005

Table 5
Comparison of monolayer adsorption capacity of CDEL with other biochars used for MB adsorption.

Biochar	Carbonisation temperature (°C)	Monolayer adsorption capacity, q_0 (mg/g)	References
Wheat straw	200	46.6	[54]
Cedrela odorata L. seed	400	158.50	[55]
Wodyetia bifurcata	700	149.30	[56]
Cattle manure	200	192.30	[57]
Anaerobic granular sludge	650	90.91	[58]
Sewage sludge	550	24.10	[59]
Sawdust	450	27.47	[60]
Magnolia grandiflora L. fallen leaf	500	65.30	[61]
Dacryodes edulis leaf	250	7.91	This study

3.9. Comparison with other biochar biosorbents

CDEL biosorption are compared with biosorption tests from other works, Table 4. Though *Wodyetia bifurcata* and anaerobic granular sludge biosorbents were prepared at 700 and 650 °C respectively [3,5], biosorbents were prepared at 200 °C for wheat straw and cattle manure biochars [1,4]. The biochar temperature conditions for wheat straw and cattle manure surface are similar to 250 °C for CDEL production. Table 4 shows that the adsorption capacity values of biochar biosorbents compared are better than that for CDEL, however, the removal efficiency of MB by CDEL was 93% at pH 4. Table 5.

4. Conclusions

This study presents CDEL a promising biosorbent for the removal of methylene blue from aqueous solution with very good performance. The following concluding points can be drawn from this study:

- CDEL dosage and time has increasing effects on MB removal from aqueous solutions while pH and temperature has negative effects.
- Removal of MB from aqueous solutions by CDEL's phytochemicals was influenced by functional groups on the surfaces, as revealed by FTIR studies.
- The equilibrium data fitted well to Freundlich Isotherms.
- Kinetic studies suggest that MB biosorption onto CDEL was by chemisorption and diffusion mechanisms.
- Thermodynamic studies reveal that MB biosorption on CDEL was exothermic and spontaneous.
- The re-usability CDEL for MB biosorption showed that ethanol is a better regeneration agent than water and that CDEL is re-usable for up to three times.

Based on obtained results, it can be concluded that CDEL is an efficient and effective biosorbent for MB removal from aqueous solutions. CDEL was derived from the leaf of *D. edulis*, an agro waste material widely cultivated, therefore it is easily available and economical, therefore, it is recommended as an alternative biosorbent for MB removal from aqueous solutions.

Ethical Approval

There were no human and animal studies.

CRediT authorship contribution statement

Nnaemeka J.N. Nnaji: Conceptualization, Writing – original draft, Investigation, Data curation, Validation, Formal analysis. **Christopher U. Sonde, Obianuju L. Nwanji, Abraham U. Onuigbo, Precious C. Mbah** and **Adamma M. Ojukwu:** Data curation, Validation, Formal analyses. **Godwin C. Ezeh:** Data curation, Validation. **Abosede Omowumi Adewumi, Edith C. Unoka and Jude O. Otedo:** Data curation, Validation. **Thereasa U. Onuegbu:** Writing – review & editing, Supervision.

Declaration of Competing Interest

The authors declare that they have no known competing financial interests or personal relationships that could have appeared to influence the work reported in this paper.

Data Availability

Data will be made available on request.

Acknowledgement

Nnaji, N.J.N. wishes to acknowledge with thanks the Department of Chemistry, Alex Ekwueme Federal University Ndufu Alike Ikwo (FUNAI) for the provision of research facilities for this work. Dr Nnaji greatly appreciates with thanks, the technical assistance Mrs Rachael Otu rendered.

Funding declaration

This is not applicable.

Appendix A. Supporting information

Supplementary data associated with this article can be found in the online version at doi:10.1016/j.jece.2023.109638.

References

[1] J.U. Ani, N.J.N. Nnaji, O.D. Onukwuli, C.O.B. Okoye, Nephelometric and functional parameters response of coagulation for the purification of industrial wastewater using Detarium microcarpum, J. Hazard. Mater. vol. 243 (. 2012) 59–66, https://doi.org/10.1016/j.jhazmat.2012.09.069.
[2] F. Deniz, Dye removal by almond shell residues: Studies on biosorption performance and process design, Mater. Sci. Eng. C. vol. 33 (5) (2013) 2821–2826, https://doi.org/10.1016/j.msec.2013.03.009.
[3] N.J. Nnaji, et al., Cashew nut testa tannin resin – preparation, characterization and adsorption studies, J. Taibah Univ. Sci. vol. 15 (1) (2021) 170–183, https://doi.org/10.1080/16583655.2021.1930717.
[4] K. Bharathi, S. Ramesh, Removal of dyes using agricultural waste as low-cost adsorbents: a review, Appl. Water Sci. vol. 3 (2013) 773–790, https://doi.org/10.1007/s13201-013-0117-y.

[5] M. Oz, D.E. Lorke, M. Hasan, G.A. Petroianu, ChemInform Abstract: Cellular and Molecular Actions of Methylene Blue in the Nervous System (p. no-no), ChemInform vol. 42 (16) (2011), https://doi.org/10.1002/chin.201116243.

[6] M. Grayling, C.D. Deakin, Methylene blue during cardiopulmonary bypass to treat refractory hypotension in septic endocarditis, J. Thorac. Cardiovasc. Surg. vol. 125 (2) (2003) 426–427, https://doi.org/10.1067/mtc.2003.140.

[7] R.S. Khokhar, M. Aqil, T. Al-Zahrani, A. Gelidan, K. Al Khayal, Novel management of methylene blue extravasation: A case report and review of literature, Saudi J. Anaesth. vol. 9 (2) (2015) 211–213, https://doi.org/10.4103/1658-354X.152891.

[8] J. Crooks, Short reports Haemolytic jaundice in methylene blue after intra-amniotic injection of, pp. 872–874, 1982.

[9] N. Goluboff, R. Wheaton, Methylene blue induced cyanosis and acutehemolytic anemia complicating the treatment of methemoglobinemia, J. Pediatr. vol. 58 (1) (1961) 86–89, https://doi.org/10.1016/S0022-3476(61)80064-4.

[10] K.A. Adegoke, O.S. Bello, Dye sequestration using agricultural wastes as adsorbents, Water Resour. Ind. vol. 12 (2015) 8–24, https://doi.org/10.1016/j.wri.2015.09.002.

[11] T. Shindhal, et al., A critical review on advances in the practices and perspectives for the treatment of dye industry wastewater, Bioengineered vol. 12 (1) (2021) 70–87, https://doi.org/10.1080/21655979.2020.1863034.

[12] S. Samsami, M. Mohamadi, M.H. Sarrafzadeh, E.R. Rene, M. Firoozbahr, Recent advances in the treatment of dye-containing wastewater from textile industries: Overview and perspectives, Process Saf. Environ. Prot. vol. 143 (2020) 138–163, https://doi.org/10.1016/j.psep.2020.05.034.

[13] T. Adane, A.T. Adugna, E. Alemayehu, Textile industry effluent treatment techniques, J. Chem. vol. 2021 (2021), https://doi.org/10.1155/2021/5314404.

[14] P.S. Vankar, R. Sarswat, A.K. Dwivedi, R.S. Sahu, An assessment and characterization for biosorption efficiency of natural dye waste, J. Clean. Prod. vol. 60 (2013) 65–70, https://doi.org/10.1016/j.jclepro.2011.09.021.

[15] S. Irem, et al., Enhanced removal of reactive navy blue dye using powdered orange waste, Ecol. Eng. vol. 58 (2013) 399–405, https://doi.org/10.1016/j.ecoleng.2013.07.005.

[16] D.S. Paz, et al., Use of papaya seeds as a biosorbent of methylene blue from aqueous solution, Water Sci. Technol. vol. 68 (2) (2013) 441–447, https://doi.org/10.2166/wst.2013.185.

[17] E.I. Unuabonah, G.U. Adie, L.O. Onah, O.G. Adeyemi, Multistage optimization of the adsorption of methylene blue dye onto defatted Carica papaya seeds, Chem. Eng. J. vol. 155 (3) (2009) 567–579, https://doi.org/10.1016/j.cej.2009.07.012.

[18] K.V. Kumar, K. Porkodi, Mass transfer, kinetics and equilibrium studies for the biosorption of methylene blue using Paspalum notatum, J. Hazard. Mater. vol. 146 (1–2) (2007) 214–226, https://doi.org/10.1016/j.jhazmat.2006.12.010.

[19] V. Ponnusami, V. Gunasekar, S.N. Srivastava, Kinetics of methylene blue removal from aqueous solution using gulmohar (Delonix regia) plant leaf powder: Multivariate regression analysis, J. Hazard. Mater. vol. 169 (1–3) (2009) 119–127, https://doi.org/10.1016/j.jhazmat.2009.03.066.

[20] G.O. El-sayed, Removal of methylene blue and crystal violet from aqueous solutions by palm kernel fibre, Desalination vol. 272 (1–3) (2018) 225–232, https://doi.org/10.1016/j.desal.2011.01.025.

[21] D. Özer, G. Dursun, A. Özer, Methylene blue adsorption from aqueous solution by dehydrated peanut hull, J. Hazard. Mater. vol. 144 (1–2) (2007) 171–179, https://doi.org/10.1016/j.jhazmat.2006.09.092.

[22] M. Doğan, H. Abak, M. Alkan, Adsorption of methylene blue onto hazelnut shell: Kinetics, mechanism and activation parameters, J. Hazard. Mater. vol. 164 (1) (2009) 172–181, https://doi.org/10.1016/j.jhazmat.2008.07.155.

[23] F.A. Pavan, A.C. Mazzocato, Y. Gushikem, Removal of methylene blue dye from aqueous solutions by adsorption using yellow passion fruit peel as adsorbent, Bioresour. Technol. vol. 99 (8) (2008) 3162–3165, https://doi.org/10.1016/j.biortech.2007.05.067.

[24] Y. Bulut, H. Aydin, A kinetics and thermodynamics study of methylene blue adsorption on wheat shells, Desalination vol. 194 (1–3) (2006) 259–267, https://doi.org/10.1016/j.desal.2005.10.032.

[25] S. Shakoor, A. Nasar, Removal of methylene blue dye from artificially contaminated water using Citrus limetta peel waste as a very low cost adsorbent, J. Taiwan Inst. Chem. Eng. vol. 66 (2016) 154–163, https://doi.org/10.1016/j.jtice.2016.06.009.

[26] R. Karthik, R. Muthezhilan, A. Jaffar Hussain, K. Ramalingam, V. Rekha, Effective removal of methylene blue dye from water using three different low-cost adsorbents, Desalin. Water Treat. vol. 57 (23) (2016) 10626–10631, https://doi.org/10.1080/19443994.2015.1039598.

[27] A. Yazidi, M. Atrous, F.E. Soetaredjo, L. Sellaoui, S. Ismadji, A. Erto, A. Bonilla-Petriciolet, G.L. Dotto, A.B. Lamine, Adsorption of amoxicillin and tetracycline on activated carbon prepared from durian shell in single and binary systems: experimental study and modeling analysis, Chem. Eng. J. vol. 379 (2020), 122320, https://doi.org/10.1016/j.cej.2019.122320.

[28] P.S. Thue, G.S. dos Reis, E.C. Lima, J.M. Sieliechi, G.L. Dotto, A.G.N. Wamba, S.L. P. Dias, F.A. Pavan, Activated carbon obtained from sapelli wood sawdust by microwave heating for o-cresol adsorption, Res. Chem. Intermed. vol. 43 (2017) 1063–1087, https://doi.org/10.1007/s11164-016-2683-8.

[29] P.R. Yaashikaa, P.S. Kumar, S. Varjani, A. Saravanan, A critical review on the biochar production techniques, characterization, stability and applications for circular bioeconomy, Biotechnol. Rep. vol. 28 (2020), e00570, https://doi.org/10.1016/j.btre.2020.e00570.

[30] J.W. Gabhane, V.P. Bhange, P.D. Patil, S.T. Bankar, S. Kumar, Recent trends in biochar production methods and its application as a soil health conditioner: a review, SN Appl. Sci. vol. 2 (7) (2020) 1–21, https://doi.org/10.1007/s42452-020-3121-5.

[31] K.K. Ajibesin, *Dacryodes edulis* (G. Don) H.J. Lam: a review on its medicinal, phytochemical and economical properties, Res. J. Med. Plants vol. 5 (1) (2010) 32–41.

[32] T.T. Olivier, F. Moïse, S.A. Jackson, N.T. Francis, A review on traditional uses, phytochemical and pharmacological profiles, spiritual and economic values, and toxicity of *Dacryodes edulis* (G. Don) H.J. Lam, J. Drug Del. Ther. vol. 6 (5) (2016) 84–90.

[33] N.J.N. Nnaji, T.U. Onuegbu, O. Edokwe, G.C. Ezeh, A.P. Ngwu, An approach for the reuse of *Dacryodes edulis* leaf: characterization, acetylation and crude oil sorption studies, J. Environ. Chem. Eng. vol. 4 (3) (2016) 3205–3216, https://doi.org/10.1016/j.jece.2016.06.010.

[34] L. Leng, Q. Xiong, L. Yang, H. Li, Y. Zhou, W. Zhang, S. Jiang, H. Li, H. Huang, An overview on engineering the surface area and porosity of biochar, Sci. Total Environ. vol. 763 (2021), 144204.

[35] G. Todou, G. Coppens d'Eeckenbrugge, H.I. Joly, A. Akoa, J.M. Onana, G. Achoundong, Climatic niche of *Dacryodes edulis* (G. Don) H.J. Lam (Burseraceae), a semi-domesticated fruit tree native to Central Africa, J. Ecol. Nat. Environ. vol. 5 (9) (2013) 231–240, https://doi.org/10.5897/JENE12.075.

[36] W. Suliman, J.B. Harsh, N.I. Abu-Lail, A.M. Fortuna, I. Dallmeyer, M. Garcia-Pérez, The role of biochar porosity and surface functionality in augmenting hydrologic properties of a sandy soil, Sci. Total Environ. vol. 574 (2017) 139–147.

[37] W. Wang, D. Lia, S. Zuo, Z. Guan, H. Xu, S. Ding, D. Xia, Discarded-leaves derived biochar for highly efficient solar water evaporation and clean water production: the crucial roles of graphitized carbon, Colloids Surf. A: Physicochem. Eng. Asp. vol. 639 (2022), 128337.

[38] M. Akmal, T.A. Gondal, K.S. Khan, Q. Hussain, M. Ahmad, M.S. Abbas, H.U. Rafa, S.A. Khosa, Impact of biochar prepared from leaves of Populous euphratica on soil microbial activity and mung bean (Vigna radiata) growth, Arab. J. Geosci. vol. 12 (2019) 591.

[39] M.J. Bentley, R.S. Summers, Ash pretreatment of pine and biosolids produces biochars with enhanced capacity for 2 organic micropollutant removal from surface water, wastewater, and stormwater, Environ. Sci.: Water Res. Technol. vol. 6 (2020) 635–644, https://doi.org/10.1039/c9ew00862d.

[40] F.A. Dawodu, K.G. Akpomie, Simultaneous adsorption of Ni(II) and Mn(II) ions from aqueous solution unto a Nigerian kaolinite clay, J. Mater. Res. Technol. vol. 3 (2) (2014) 129–141, https://doi.org/10.1016/j.jmrt.2014.03.002.

[41] S.T. Akar, D. Yilmazer, S. Celik, Y.Y. Balk, T. Akar, On the utilization of a lignocellulosic waste as an excellent dye remover: Modification, characterization and mechanism analysis, Chem. Eng. J. vol. 229 (2013) 257–266, https://doi.org/10.1016/j.cej.2013.06.009.

[42] A.A. Welch, et al., Variation in intakes of calcium, phosphorus, magnesium, iron and potassium in 10 countries in the european prospective investigation into cancer and nutrition study, Eur. J. Clin. Nutr. vol. 63 (2009) S101–S121, https://doi.org/10.1038/ejcn.2009.77.

[43] M. Özacar, I.A. Şengil, Adsorption of metal complex dyes from aqueous solutions by pine sawdust, Bioresour. Technol. vol. 96 (7) (2005) 791–795, https://doi.org/10.1016/j.biortech.2004.07.011.

[44] J.O. Ighalo, K.O. Iwuozor, C.A. Igwegbe, A.G. Adeniyi, Verification of pore size effect on aqueous-phase adsorption kinetics: a case study of methylene blue, Colloids Surf. A: Physicochem. Eng. Asp. vol. 626 (2021), 127119.

[45] L.K. Kian, M. Jawaid, Thermal properties of nanocrystalline cellulose and cellulose nanowhisker, Int. J. Innov. Technol. Explor. Eng. vol. 9 (1) (2019) 5430–5434, https://doi.org/10.35940/ijitee.A8103.119119.

[46] R.A.C. Gomide, A.C.S. de Oliveira, D.A.C. Rodrigues, C.R. de Oliveira, O.B.G. de Assis, M.V. Dias, S.V. Borges, Development and characterization of lignin microparticles for physical and antioxidant enhancement of biodegradable polymers, J. Polym. Environ. vol. 28 (2020) 1326–1334.

[47] C.U. Sonde, N. Nnaji, S.A. Odoemelam, F.K. Ekuma, G.C. Ezeh, C.P. Okoli, "Methylene blue removal by agricultural wastes from Annona muricata and Treculia africana seeds," Biomass Conversion and Biorefnery (Accepted) doi: 10.1007/s13399–022-03419–8.

[48] W. Kim, C.Y. Suh, S.W. Cho, K.M. Roh, H. Kwon, K.S.J. Shon, A new method for the identification and quantification of magnetite–maghemite mixture using conventional X-ray diffraction technique, Talanta vol. 94 (2012) 348–352.

[49] S.J. Allen, Q. Gan, R. Matthews, P.A. Johnson, Comparison of optimised isotherm models for basic dye adsorption by kudzu, Bioresour. Technol. vol. 88 (2) (2003) 143–152, https://doi.org/10.1016/S0960-8524(02)00281-X.

[50] E.I. Unuabonah, B.I. Olu-Owolabi, K.O. Adebowale, A.E. Ofomaja, Adsorption of lead and cadmium ions from aqueous solutions by tripolyphosphate-impregnated Kaolinite clay, Colloids Surf. A Physicochem. Eng. Asp. vol. 292 (2–3) (2007) 202–211, https://doi.org/10.1016/j.colsurfa.2006.06.024.

[51] P. García-Pérez, S. Losada-Barreiro, P.P. Gallego, C. Bravo-Díaz, Adsorption of gallic acid, propyl gallate and polyphenols from Bryophyllum extracts on activated carbon, Sci. Rep. vol. 9 (2019) 14830, https://doi.org/10.1038/s41598-019-51322-6.

[52] B.H. Hameed, Removal of cationic dye from aqueous solution using jackfruit peel as non-conventional low-cost adsorbent, J. Hazard. Mater. vol. 162 (2009) 344–350, https://doi.org/10.1016/j.jhazmat.2008.05.045.

[53] S.S. Rani, R.K. Mahajan, Equilibrium, kinetics and thermodynamic parameters for adsorptive removal of dye Basic Blue 9 by ground nut shells and Eichhornia, Arab. J. Chem. vol. 9 (2016) S1464–S1477, https://doi.org/10.1016/j.arabjc.2012.03.013.

[54] G. Li, W. Zhu, C. Zhang, S. Zhang, L. Liu, L. Zhu, W. Zhao, Effect of a magnetic field on the adsorptive removal of methylene blue onto wheat straw biochar, Bioresour. Technol. vol. 206 (2016) 16–22, https://doi.org/10.1016/j.biortech.2015.12.087.

[55] A. Subratti, J. Ladeira, L.J. Lalgee, F.M. Kerton, N.K. Jalsa, Preparation and characterization of biochar derived from the fruit seed of Cedrela odorata L and evaluation of its adsorption capacity with methylene blue, Sustain. Chem. Pharm. vol. 21 (2021), 100421, https://doi.org/10.1016/j.scp.2021.100421.
[56] K.J.L. dos Santos, G.E. de Souza dos Santos, Í.M.G.L. de Sá, A.H. Ide, J.L. da Silva Duarte, S.H.V. de Carvalho, J.I. Soletti, L. Meili, *Wodyetia bifurcata* biochar for methylene blue removal from aqueous matrix, Bioresour. Technol. vol. 293 (2019), 122093, https://doi.org/10.1016/j.biortech.2019.122093.
[57] Y. Zhu, B. Yi, S. Yan, Q. Yuan, and Y. Wu, Removal of methylene blue from aqueous solution by cattle manure-derived low temperature biochar, pp. 19917–19929, 2018, doi: 10.1039/c8ra03018a.
[58] L. Shi, G. Zhang, D. Wei, T. Yan, X. Xue, S. Shi, Q. Wei, Preparation and utilization of anaerobic granular sludge-based biochar for the adsorption of methylene blue from aqueous solutions, J. Mol. Liq. vol. 198 (2014) 334–340, https://doi.org/10.1016/j.molliq.2014.07.023.
[59] S. Fan, Y. Wang, Z. Wang, J. Tang, J. Tang, X. Li, Removal of methylene blue from aqueous solution by sewage sludge-derived biochar: Adsorption kinetics, equilibrium, thermodynamics and mechanism, Biochem. Pharmacol. vol. 5 (2017) 601–611, https://doi.org/10.1016/j.jece.2016.12.019.
[60] H. Nath, A. Saikia, P. Jyoti, B.K. Saikia, N. Saikia, Removal of methylene blue from water using okra (Abelmoschus esculentus L.) mucilage modified biochar, Bioresour. Technol. Rep. vol. 14 (2021), 100689, https://doi.org/10.1016/j.biteb.2021.100689.
[61] B. Ji, J. Wang, H. Song, W. Chen, Removal of methylene blue from aqueous solutions using biochar derived from a fallen leaf by slow pyrolysis: behavior and mechanism, J. Environ. Chem. Eng. vol. 7 (3) (2019), 103036, https://doi.org/10.1016/j.jece.2019.103036.